

Dark SU(2) states of the motion of a trapped ion

Z. Kis,^{1,*} W. Vogel,¹ L. Davidovich,² and N. Zagury²

¹*Arbeitsgruppe Quantenoptik, Fachbereich Physik, Universität Rostock, Universitätsplatz 3, D-18051 Rostock, Germany*

²*Instituto de Física, Universidade Federal de Rio de Janeiro, Caixa Postal 68528, 21945-970 Rio de Janeiro, RJ, Brazil*

(Received 14 June 2000; published 16 April 2001)

The preparation of SU(2) states as dark states of the motion of a trapped ion is considered. The difficulty in preparing these states is shown to arise from the degeneracy of eigenvalues of the Hamiltonian. This degeneracy is removed by making use of the nonlinearities appearing in the dynamics of an ion that is not well localized. The mechanism of approaching the dark state of interest is analyzed by using the quantum trajectory method.

DOI: 10.1103/PhysRevA.63.053410

PACS number(s): 32.80.Pj, 42.50.Vk, 32.80.Qk, 42.50.Lc

I. INTRODUCTION

During the last few decades ion traps have become a prominently important tool for studying fundamental quantum-mechanical phenomena. In an ion trap the center-of-mass of a single ion experiences an approximate harmonic external potential [1], hence the ion trap is a realization of the harmonic-oscillator model in quantum mechanics. Ion trapping inspired the development of laser cooling techniques such as ‘‘Doppler’’ laser cooling [2–4], and laser cooling in the resolved sideband limit [4], which allows one to prepare the ion in the vibrational ground state [5,6]. Making use of the momentum exchange between atom and light, one can manipulate the atomic center-of-mass motion. In this manner, experiments have been performed to generate motional number states, squeezed states [7], and Schrödinger-catlike states [8].

Several nonclassical states are very sensitive to decoherence effects that limit their lifetimes. It may be advantageous to generate the target vibrational state in such a way that even in the presence of noise the disturbed system evolves back to the target state. This will happen if this state is an eigenstate of the interaction Hamiltonian with zero eigenvalue, which is not affected by dissipation. The latter requirement is achieved, in particular, when the atom is in the ground state, so that spontaneous decay is not allowed. Fluorescence disappears, leading to a ‘‘dark’’ state. There have been several theoretical proposals dealing with motional dark states that realize this type of dynamics, including squeezed states [9], even and odd coherent states [10], nonlinear coherent states [11], and squeezed cat states [12]. Similarly, the generation of multimode entangled states as dark states could also be of practical importance. In this spirit, the preparation of pair coherent states [13] and pair cat states [14] has already been considered.

In this paper we show that it is possible to generate dark SU(2) states of the center-of-mass motion of a trapped ion. These are entangled states of the vibrations along two orthogonal trap directions, which can be characterized by quantum numbers corresponding to pseudoangular momen-

tum operators. These operators are defined in terms of bilinear combinations of the bosonic operators corresponding to the two directions, using the Schwinger representation [15]. Some particular properties, including the generation and the detection of pseudoangular momentum states of the motion of a trapped ion have been discussed in Ref. [16]. We show that it is possible to engineer, with properly tuned laser beams, interaction Hamiltonians with zero-energy eigenstates that are very good approximations to SU(2) vibrational states. We also show that, for each of these Hamiltonians, the zero-energy eigenvalue must be nondegenerate in order to have a stable dark state. This requires exploiting the nonlinearities of the laser-ion interaction.

The paper is organized as follows: In Sec. II the excitation scheme is considered and the effective Hamiltonian is given. The properties of the eigensystem of the Hamiltonian are studied in Sec. III, with particular emphasis on the effect of the nonlinear character of the interaction on the degeneracy of the eigenvalues. The dynamical evolution of the system is considered in Sec. IV. Section V is devoted to analyze the mechanism of how the system approaches the motional dark state. A summary and some conclusions are given in Sec. VI.

II. THE HAMILTONIAN

In this section we discuss the physical model of the experimental setup that realizes the dynamics under consideration. An ion is trapped in a rf Paul trap where we concentrate on the two-dimensional motion of the ion [17]. The ion is considered as an effective electronic two-level system. The electronic transition is driven by three resonant laser fields; one of them is tuned to the carrier frequency, the others are tuned to vibrational sidebands, see Fig. 1. The Hamiltonian of the system in the electronic rotating wave approximation reads

$$\hat{H} = \hat{H}_0 + \hat{H}_{\text{int}}(t), \quad (1)$$

where

$$\hat{H}_0 = \hbar \omega_{21} \hat{A}_{22} + \hbar \nu_x \hat{a}^\dagger \hat{a} + \hbar \nu_y \hat{b}^\dagger \hat{b} \quad (2)$$

describes the free motion of the internal and external degrees of freedom of the ion, and

*Permanent address: Research Institute for Solid State Physics and Optics, P. O. Box 49, H-1525 Budapest, Hungary.

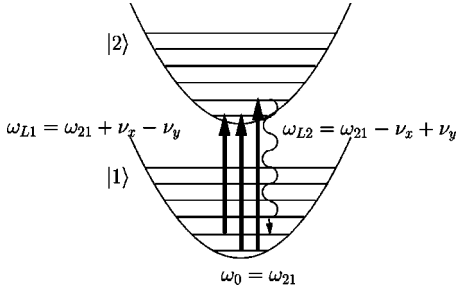


FIG. 1. Excitation scheme of the trapped ion. Three laser fields are applied, one of them is at the carrier frequency of the electronic transition, the other two are at vibrational sidebands. The wavy arrow indicates the spontaneous emission.

$$\hat{H}_{\text{int}}(t) = \frac{1}{2} [\hbar \Omega_0 e^{i(k_0 r - \omega_{21} t)} + \hbar \Omega_1 e^{i(k_1 r - \omega_{L1} t)} + \hbar \Omega_2 e^{i(k_2 r - \omega_{L2} t)}] \hat{A}_{21} + \text{H.c.} \quad (3)$$

is the interaction of the ion with the laser fields. The frequencies ν_x and ν_y describe the center-of-mass motion of the ion in the harmonic trapping potential in the x and y directions, respectively. It is assumed that $\nu_x < \nu_y$. The vibrational mode operators associated with the x and y motions are \hat{a} and \hat{b} , respectively. The electronic flip operators are denoted by \hat{A}_{ij} ($i, j = 1, 2$). Ω_i ($i = 0, 1, 2$) describes the strength of the ion-laser interaction, and the fields are characterized by the wave vectors \mathbf{k}_i ($i = 0, 1, 2$) and frequencies ω_{21} and ω_{L_i} ($i = 1, 2$). One of the lasers is tuned to the carrier frequency ω_{21} of the electronic transition. The frequency ω_{L1} is chosen in such a way that the electronic transition is accompanied by a creation of the vibrational quantum in the x mode and an annihilation of the vibrational quantum in the y mode, i.e., $\omega_{L1} = \omega_{21} + \nu_x - \nu_y$. Similarly, the frequency of the other light field driving a sideband is $\omega_{L2} = \omega_{21} + \nu_y - \nu_x$.

The Lamb-Dicke parameters are defined by

$$\eta_{iq} = \Delta q k_{iq}, \quad (4)$$

where Δq ($q = x, y$) is the spread of the vibrational ground-state wave function of the center-of-mass motion of the ion in the trap, and k_{iq} is the q th component of the wave vector of the i th laser field. We choose now the directions of propagation of the laser fields so that some of the Lamb-Dicke parameters become small. For the field at the carrier frequency we set $\eta_{0,x,y} \ll 1$. For the other two fields we choose $\eta_{i,y} \ll 1$ and define $\eta = \eta_{i,x}$.

The Hamiltonian (1) in the interaction picture with respect to \hat{H}_0 [cf. Eq. (2)] and in the vibrational rotating wave approximation reads

$$\hat{H}_I = \frac{\hbar}{2} \{ \Omega_0 - \tilde{\Omega} [f_1(\hat{n}_x; \eta) \hat{a} \hat{b}^\dagger + \hat{a}^\dagger \hat{b} f_1(\hat{n}_x; \eta)] \} \hat{A}_{21} + \text{H.c.}, \quad (5)$$

where we require that the parameters of both laser fields tuned to vibrational sidebands satisfy the condition $\tilde{\Omega} = \eta_{ix} \eta_{iy} e^{-\eta_{iy}^2/2} \Omega_i$ ($i = 1, 2$), and

$$f_1(\hat{n}; \eta) = e^{-\eta^2/2} \sum_{n=0}^{\infty} \frac{1}{n+1} L_n^{(1)}(\eta^2) |n\rangle \langle n|, \quad (6)$$

where $L_n^{(1)}(x)$ is the n th first-order associated Laguerre polynomial.

In Eq. (5), the Lamb-Dicke approximation was adopted for the y direction, and also for the carrier field in the x direction, since $\eta_{0,x,y}, \eta_{i,y} \ll 1$, and we also assume that the occupation numbers in the x and the y direction are such that $\eta_{0,x,y} \sqrt{n_x + 1} \ll 1$, $\eta_{0,x,y} \sqrt{n_y + 1} \ll 1$, and $\eta_{i,y} \sqrt{n_y + 1} \ll 1$. This approximation implies that the dependence of the interaction on \hat{n}_y is neglected. We keep however the dependence on \hat{n}_x , assuming that $\eta_{ix} = \eta$ has a larger value.

Given two independent sets of boson operators $\{\hat{a}, \hat{a}^\dagger\}$ and $\{\hat{b}, \hat{b}^\dagger\}$, one may introduce operators satisfying the angular momentum algebra in the following way [15]:

$$\begin{aligned} \hat{J}_1 &= (\hat{a}^\dagger \hat{b} + \hat{a} \hat{b}^\dagger)/2, & \hat{J}_2 &= (\hat{a}^\dagger \hat{b} - \hat{a} \hat{b}^\dagger)/2i, \\ \hat{J}_3 &= (\hat{a}^\dagger \hat{a} - \hat{b}^\dagger \hat{b})/2, & \hat{J}^2 &= \hat{J}_1^2 + \hat{J}_2^2 + \hat{J}_3^2. \end{aligned} \quad (7)$$

For the trapped ion, the two-mode Fock state $|n_x, n_y\rangle$ can be described as the pseudoangular momentum state that is a common eigenstate of the pseudoangular momentum operators \hat{J}^2 and \hat{J}_3 associated with the eigenvalues $(n_x + n_y)(n_x + n_y + 2)/4$ and $(n_x - n_y)/2$, respectively [16]. One should note that the three operators \hat{J}_i are constructed with operators corresponding to the quantized motion in the plane $x-y$. Therefore they cannot be related to the orbital angular momentum components \hat{L}_i , $i = x, y, z$, of the trapped ion. Only if $\nu_x = \nu_y$ do we have \hat{J}_2 proportional to \hat{L}_z , but even in this case the other components of \hat{J} do not have a similar interpretation.

Now we can insert the pseudoangular momentum operators (7) into Eq. (5) to obtain

$$\hat{H}_I = -\hbar \tilde{\Omega} [\hat{B}_{\text{vib}} - \mathcal{E}] \hat{A}_{21} + \text{H.c.}, \quad (8)$$

where $\mathcal{E} = \Omega_0/2\tilde{\Omega}$ and

$$\hat{B}_{\text{vib}} = \frac{1}{2} [f_1(|\hat{J}| + \hat{J}_3; \eta) \hat{J}_- + \hat{J}_+ f_1(|\hat{J}| + \hat{J}_3; \eta)], \quad (9)$$

where $\hat{J}_\pm = \hat{J}_1 \pm i\hat{J}_2$, and $|\hat{J}| = (\hat{n}_x + \hat{n}_y)/2$. It is clearly seen that \hat{B}_{vib} is a Hermitian operator. If $\eta \sqrt{n_x + 1} \ll 1$ then one may perform the Lamb-Dicke approximation in the x mode too and the operator associated with the center-of-mass motion of the ion simplifies to

$$\lim_{\eta \rightarrow 0} \hat{B}_{\text{vib}} = \hat{J}_1. \quad (10)$$

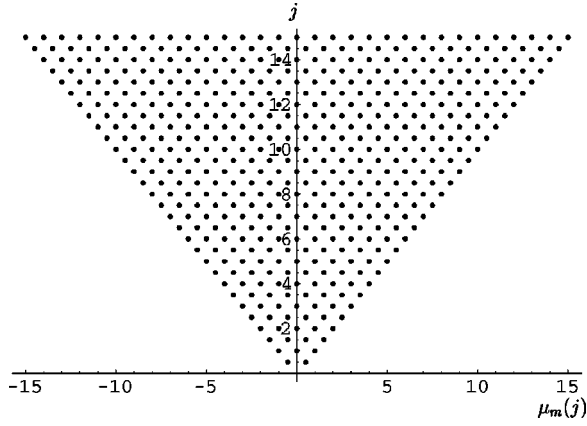


FIG. 2. The eigenvalue spectrum of \hat{B}_{vib} for $\eta \leq 1$ (j, μ_m are dimensionless). The spectrum is highly degenerate.

For large η values the vibrational operator in Eq. (9) may be considered as a nonlinear generalization of the pseudoangular momentum operator \hat{J}_1 .

III. EIGENSTATES AND EIGENVALUES

In this section we study the properties of the eigensystem of \hat{B}_{vib} . It can be easily seen that \hat{B}_{vib} commutes with \hat{J}^2 for any value of η . Consequently, the operators \hat{J}^2 and \hat{B}_{vib} possess a common eigenstate system,

$$\begin{aligned}\hat{B}_{\text{vib}}|j\mu_m\rangle &= \mu_m(j)|j\mu_m\rangle, \\ \hat{J}^2|j\mu_m\rangle &= j(j+1)|j\mu_m\rangle.\end{aligned}\quad (11)$$

For every pseudoangular momentum j there are, in general, $2j+1$ different eigenvalues $\mu_m(j)$ and the corresponding eigenstates $|j\mu_m\rangle$. The index m in μ_m signifies that in the limit $\eta \rightarrow 0$ the eigenvalue is $\mu_m = m$ and the states $|j\mu_m\rangle$ tend to the eigenstates $|jm\rangle$ of the operators \hat{J}^2 and \hat{J}_1 .

Let us consider first the limit $\eta \rightarrow 0$. Then, as seen before, the operator \hat{B}_{vib} reduces to \hat{J}_1 . The eigenvalues of \hat{J}_1 are displayed in Fig. 2. It is clearly seen that the eigenvalue spectrum is highly degenerate. The corresponding eigenstates are entangled in the Fock basis associated with the x and y axes. For example, the state corresponding to $m_1 = 1/2, j = 1/2$ is

$$|j=1/2, m_1=1/2\rangle = (|10\rangle + |01\rangle)/\sqrt{2}, \quad (12)$$

while the state with $j=1, m_1=0$ may be written as

$$|j=1, m_1=0\rangle = (|20\rangle - |02\rangle)/\sqrt{2}. \quad (13)$$

For more general types of these states see, for example Ref. [16]. Entangled states like these may play an important role in quantum information theory and in the study of quantum decoherence effects. Our aim is to obtain these entangled states as dark states, thus protecting them from degrading caused by noise. We will show in the next section that dark states should be zero-energy eigenvectors of the interaction

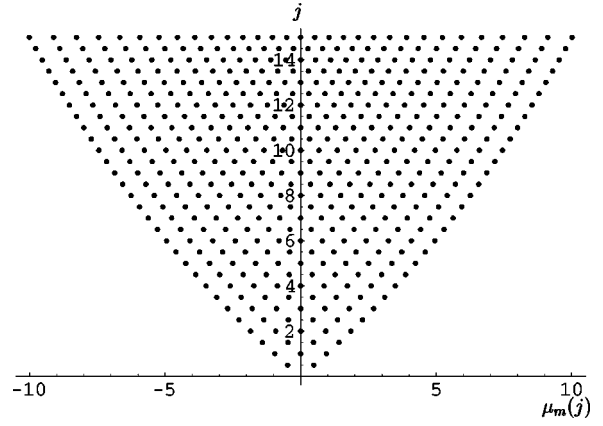


FIG. 3. The eigenvalue spectrum of \hat{B}_{vib} for $\eta=0.25$. The degeneracy is raised due to the nonlinearity.

Hamiltonian, with the ion in its ground electronic level. It is clear that, by adjusting the constant \mathcal{E} in Eq. (8), we can select the eigenspace that corresponds to the zero eigenvalue of \hat{H}_I in Eq. (8). However, in order to select a single pseudoangular momentum eigenstate, this eigenspace must be nondegenerate. This can be achieved by exploiting the nonlinearities associated with the ion-laser interaction (large enough Lamb-Dicke parameter). We will show in the next section that it is then possible to get stable target dark states, which are very good approximations to the SU(2) states mentioned before.

For a nonvanishing Lamb-Dicke parameter η the eigensystem can be calculated numerically by diagonalizing the operator (9). We call the eigenstates of \hat{B}_{vib} nonlinear pseudoangular momentum states. The degeneracy of the eigenvalue spectrum of \hat{B}_{vib} is resolved, at least for nearby eigenvalues, as clearly shown in Fig. 3. Accidental degeneracies may still occur, but they will not affect our scheme substantially if the eigenvalues involved are very far away in the diagram shown in Fig. 3.

To get some insight on how the degeneracy in the eigenvalue spectrum is raised, one may calculate approximately the difference between two eigenvalues for increasing η . For $\eta=0$ we choose the eigenvalues $\mu_{1/2}(3/2)$ and $\mu_{1/2}(1/2)$. Expanding the operator $f_1(\hat{n}; \eta)$ in \hat{B}_{vib} into a Taylor series up to second order in η , one finds

$$\mu_{1/2}(3/2) - \mu_{1/2}(1/2) = -\frac{\eta^2}{4} + \mathcal{O}(\eta^4). \quad (14)$$

Though in general the eigenvalues of \hat{B}_{vib} are different from that of \hat{J}_1 the corresponding eigenstates are still very close to each other. In Table I we show the square of the overlap of the eigenstates of \hat{J}_1 and \hat{B}_{vib} for $\eta=0.25$. It can be seen that even for this value of the Lamb-Dicke parameter the overlap is close to unity for the first few values of the total pseudoangular momentum j . It follows that by generating the eigenstates of \hat{B}_{vib} one gets states that are almost perfect SU(2) states. In the next section we discuss a dynamics that yields these states as stationary ones.

TABLE I. The overlap between the eigenstates of \hat{J}_1 and the corresponding eigenstates of \hat{B}_{vib} for $\eta=0.25$.

j	$ \langle jm j\mu_m\rangle ^2$
0	1.0000
0.5	1.0000 1.0000
1	0.9999 0.9997 0.9999
1.5	0.9992 0.9992 0.9992 0.9992
2	0.9977 0.9973 0.9992 0.9973 0.9977
2.5	0.9948 0.9928 0.9979 0.9979 0.9928 0.9948
3	0.9903 0.9844 0.9933 0.9984 0.9933 0.9844 0.9903
3.5	0.9837 0.9712 0.9834 0.9960 0.9960 0.9834 0.9712 0.9837

IV. DYNAMICAL BEHAVIOR

The time evolution of the system is characterized by the Master equation

$$\frac{d\hat{\rho}}{dt} = -\frac{i}{\hbar}[\hat{H}_I, \hat{\rho}] + \frac{\Gamma}{2}(2\hat{A}_{12}\tilde{\rho}\hat{A}_{21} - \hat{A}_{22}\hat{\rho} - \hat{\rho}\hat{A}_{22}), \quad (15)$$

where \hat{H}_I is defined in Eq. (8) and the last term describes spontaneous emission with energy relaxation rate Γ , and

$$\tilde{\rho} = \int dudv w(u,v) \exp[i\eta_x^{(r)}(\hat{a} + \hat{a}^\dagger)u + i\eta_y^{(r)}(\hat{b} + \hat{b}^\dagger)v] \hat{\rho} \times \exp[-i\eta_x^{(r)}(\hat{a} + \hat{a}^\dagger)u - i\eta_y^{(r)}(\hat{b} + \hat{b}^\dagger)v], \quad (16)$$

accounts for changes of the vibrational energy due to spontaneous emission. $w(u,v)$ is the angular distribution of spontaneous emission and $\hat{\rho}$ the vibronic density operator, reduced with respect to the vibrational motion in the z direction [17].

The stationary solution $\hat{\rho}_s$ of Eq. (15) can be found by setting $d\hat{\rho}/dt=0$ on its left-hand side. If one sets the amplitude of the laser field such that $\mathcal{E}=\mu_m(j)$ in Eq. (8), then the stationary solution is

$$\hat{\rho}_s = |1\rangle|j\mu_m\rangle\langle j\mu_m|\langle 1|, \quad (17)$$

where $|1\rangle$ is the electronic ground state and $|j\mu_m\rangle$ is a non-degenerate eigenstate of \hat{B}_{vib} defined in Eq. (11). Note that the ion stops to interact with the laser fields when it reaches the steady state and it remains in a ‘‘dark state.’’ In the following we analyze under which circumstances the dynamics governed by the Master equation (15) leads to a unique solution of the equation $d\hat{\rho}/dt=0$.

First we consider the Hamiltonian evolution. Let’s assume that there are several eigenstates $|j_i\mu_m\rangle$ which belong to the same eigenvalue $\mu_m(j_i)\equiv\mu_m$ in Eq. (11). It is clear that in this case the dynamics does not lead to a unique solution of the equation $d\hat{\rho}/dt=0$, instead it results in an incoherent superposition of the states $|1\rangle|j_i\mu_m\rangle$. The coefficients of the superposition will depend on the initial state. Consequently,

in order that an eigenvector of $|j_i\mu_m\rangle$ be the steady-state solution of Eq. (15), the operator \hat{B}_{vib} must have a nondegenerate eigenvalue spectrum.

If the Lamb-Dicke parameter η is sufficiently large, this condition is fulfilled, except for the possible presence of accidental degeneracies, see the discussion in the previous section. These degeneracies in the eigenvalues of the operator \hat{B}_{vib} will not change the results substantially, as long as the involved eigenvalues of \hat{J}^2 are well separated, and if the initial state belongs to a subspace that is close to one of the degenerate eigenstates and far away from the other. Then, the probability of populating the ‘‘undesired’’ state remains very small.

Let’s assume that the initial state of the system is a pure state $|\psi\rangle_{\text{in}}$. This state can be expanded as a superposition of the eigenstates of \hat{B}_{vib}

$$|\psi\rangle_{\text{in}} = |1\rangle \sum_{j\mu_m} c_{j\mu_m} |j\mu_m\rangle. \quad (18)$$

The Hamiltonian evolution connects only states having the same pseudoangular momentum. Therefore for approaching a target state $|1\rangle|j'\mu'_m\rangle$, the non-Hermitian part in the Master equation (15) plays an important role.

We have performed quantum trajectory simulations [18–20] to understand this evolution. The effective, non-Hermitian Hamiltonian governing the continuous dynamics reads

$$\hat{H}_{\text{eff}} = \hat{H}_I - i\frac{\hbar\Gamma}{2}\hat{A}_{22}, \quad (19)$$

where \hat{H}_I is defined in Eq. (8) and the jump operators are given by

$$\hat{J}_{uv} = \sqrt{\Gamma w(u,v)} \hat{A}_{12} \exp[iuk_{21}\hat{x}(t) + ivk_{21}\hat{y}(t)]. \quad (20)$$

In the course of quantum trajectory simulations an initial wave function is evolved with the Hamiltonian \hat{H}_{eff} , and jumps at random times, interrupt this evolution. The times of the jumps are determined by the decay of the norm of the time-evolved wave function.

V. APPROACHING THE DARK STATE

Let us consider the approach of the system to the required target state by the use of the quantum trajectory method. The conditional wave function of the system is

$$|\psi\rangle = |1\rangle|\psi_1\rangle + |2\rangle|\psi_2\rangle, \quad (21)$$

where $|i\rangle$ denotes the electronic state and $|\psi_i\rangle$ is the corresponding vibrational state. $|\psi_i\rangle$ can be expanded into a series of the eigenstates of \hat{B}_{vib}

$$|\psi_1\rangle = \sum_{j\mu_m} c_{j\mu_m} |j\mu_m\rangle, \quad |\psi_2\rangle = \sum_{j\mu_m} d_{j\mu_m} |j\mu_m\rangle. \quad (22)$$

The continuous time evolution of the coefficients $c_{j\mu_m}$ and $d_{j\mu_m}$ is determined by the equations

$$\begin{aligned} \dot{c}_{j\mu_m} &= -i\tilde{\Omega}(\mu_m - \mu'_n)d_{j\mu_m}, \\ \dot{d}_{j\mu_m} &= -i\tilde{\Omega}^*(\mu_m - \mu'_n)c_{j\mu_m} - \frac{\Gamma}{2}d_{j\mu_m}, \\ j &= 0, \frac{1}{2}, 1, \dots, -j \leq m \leq +j, \end{aligned} \quad (23)$$

where μ'_n is the eigenvalue corresponding to the vibrational part $|j'\mu'_n\rangle$ of the target state. If $\mu_m \neq \mu'_n$, then in a long timescale without jumps, the solution of Eq. (23) is $c_{j\mu_m} = d_{j\mu_m} = 0$. In the special case $j = j'$ and $m = n$ one has

$$\dot{c}_{j'\mu'_n} = 0, \quad \dot{d}_{j'\mu'_n} = -\frac{\Gamma}{2}d_{j'\mu'_n}. \quad (24)$$

The probability amplitude $c_{j'\mu'_n}$ of the target state is conserved. This equation clearly shows that if in the initial state the weight of the target state is zero, then only the jumps may lead to the target state $|1\rangle|j'\mu'_n\rangle$.

Let's study the effect of the jumps. The initial state is assumed to be $|\psi(0)\rangle = |1\rangle|\psi_1\rangle$. As a simplest model we ignore for the moment the motional kick effects and assume that the jump operator (20) acts vertically, i.e., $\hat{J}_{uv} = \sqrt{\Gamma w(u,v)}\hat{A}_{12}$. This corresponds to a small Lamb-Dicke parameter associated with the spontaneous emission. When a jump occurs the following transformation is applied:

$$c_{j\mu_m}^{(+)} = d_{j\mu_m}^{(-)} \quad \text{and} \quad d_{j\mu_m}^{(+)} = 0 \quad (25)$$

for all allowed indices (j, m) , and the state vector should be renormalized. The superscripts $(-)/(+)$ indicate the coefficients just before or after a jump. The first jump occurs when the norm of the conditional wave function (21) gets smaller than a previously drawn random number ε . If the probability amplitude of the target state is $c_{j'\mu'_n}$ in the initial state then the norm of the conditional wave function can never become smaller than $p_{\text{no}} = |c_{j'\mu'_n}|^2$ since this quantity is conserved according to Eq. (24). Consequently if $\varepsilon < p_{\text{no}}$ then in a long timescale the state of the system will be the wanted target state since all the other coefficients vanish according to Eq. (23). Performing several runs one has p_{no} probability that the first drawn random number is smaller than p_{no} . It follows that in the long timescale the density operator associated with the vibrational degree of freedom is

$$\hat{\rho}_{\text{vib}}(t) = p_{\text{no}}|j'\mu'_n\rangle\langle j'\mu'_n| + (1 - p_{\text{no}})\hat{\rho}'(t)_{\text{vib}}, \quad (26)$$

where $\hat{\rho}'(t)_{\text{vib}}$ is a density operator that has no projection onto the state $|j'\mu'_n\rangle$. Consequently, in this case the dynamics does not lead to the required target state but it results in a mixed state in which the weight of the target state is p_{no} .

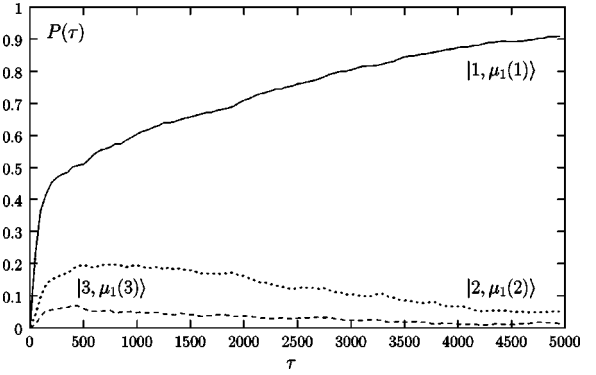


FIG. 4. The variation of some populations determined from the time evolved density operator $\hat{\rho}(t)$. The target state is $|1\rangle|1, \mu_1(1)\rangle$. Time is measured in $1/\Gamma$ units, $\tau = \Gamma t$ (dimensionless). The curves are obtained by averaging 750 trajectories.

In a real trap the Lamb-Dicke parameters associated with the spontaneous emission are so large that one cannot replace the exponential factor by 1 in the jump operators \hat{J}_{uv} , Eq. (20). The role of the exponential part is to mix vibrational states of different indices, i.e., the jumps are nonvertical. The matrix elements of the exponential term in \hat{J}_{uv} are

$$D_{j\mu_m; k\mu_n}^{(uv)} = \langle j\mu_m | \exp [i\eta_x^{(r)}(\hat{a} + \hat{a}^\dagger)u + i\eta_y^{(r)}(\hat{b} + \hat{b}^\dagger)v] | k\mu_n \rangle, \quad (27)$$

which is in general a nondiagonal matrix. Consequently, in place of the vertical transitions given in Eq. (25), the vibrational distribution transforms now as

$$c_{j\mu_m}^{(+)} = \sum_{k\mu_n} D_{j\mu_m; k\mu_n}^{(uv)} d_{k\mu_n}^{(-)}, \quad d_{j\mu_m}^{(+)} = 0 \quad (28)$$

for all allowed indices (j, m) , and the state vector should be renormalized. These considerations show clearly that the speed of approaching a required target state depends on the magnitude of the Lamb-Dicke parameters $\eta_{x,y}^{(r)}$ associated with the spontaneous emission. In the quantum trajectory simulation one trajectory is a sequence of free evolutions described by Eq. (23) and jumps according to Eq. (28). After a jump the probability amplitude $c_{j'\mu'_n}$ of the target state is given by Eq. (28). If the next drawn random number is smaller than $|c_{j'\mu'_n}|^2$, then after some time the dynamical evolution stops and the system remains in the target state $|1\rangle|j'\mu'_n\rangle$. According to the discussion in the previous section this state is a dark state since in this state the ion is decoupled from the driving laser fields and it stops to radiate.

In our first numerical example the eigenvalue $\mu_1(1)$ was chosen for \mathcal{E} in the interaction Hamiltonian in Eq. (8). Therefore the target state is $|1\rangle|1, \mu_1(1)\rangle$. The initial state was $|\psi(0)\rangle = |1\rangle|00\rangle$. In order to study the time evolution of the density operator, the variations of some populations are plotted in Fig. 4. The actual values of the Lamb-Dicke parameters were chosen in such a way that the time needed to reach the steady state is reasonably short: $\eta = 0.25$, $\eta_x^{(r)} = 0.6$, and $\eta_y^{(r)} = 0.2$. The effective interaction strength was set to $\tilde{\Omega}$

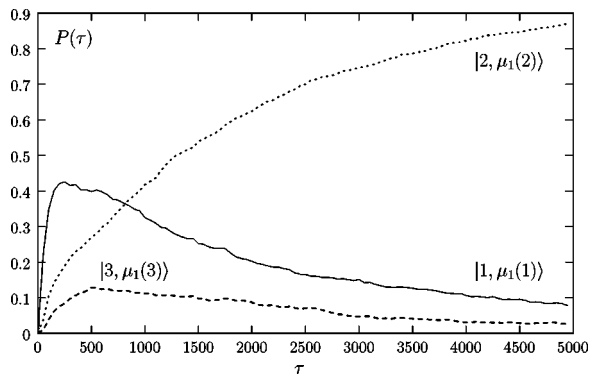


FIG. 5. Same as Fig. 4 but the target state is $|1\rangle|2, \mu_1(2)\rangle$.

$=2\Gamma$. The continuous curve corresponds to the target state. The two other curves are associated with states that have eigenvalues that are very close to that of the target state. The time evolution consists of two parts. In the beginning the population of the target state increases rapidly. After a certain time interval this quick growth is slowed down significantly. Around the end of the rapid growth there are other nondesired states, which are also populated significantly. It can be seen that a long time is needed to depopulate these states and to get all the population in the target state.

In the second numerical simulation \mathcal{E} was set to $\mu_1(2)$ in Eq. (8). The Lamb-Dicke parameters were the same as in the previous example. In Fig. 5 the populations of the same states are shown as in Fig. 4. The dynamics consists of two stages again. At the end of the first part the populations of the chosen states are similar to those in the previous case. The state $|1, \mu_1(1)\rangle$ has the highest population. In the slow period the population of this state together with the state $|3, \mu_1(3)\rangle$ decreases while the population of the state $|2, \mu_1(2)\rangle$ approaches unity.

VI. SUMMARY AND CONCLUSION

We have worked out a scheme to prepare dark SU(2) vibrational states of a trapped ion. In the scheme an electronic transition of an ion is driven by running wave laser fields. Two laser fields realize the pseudoangular momentum

Hamiltonian, while a third one sets an eigenvalue. It has been shown that, in the Lamb-Dicke regime, pure pseudoangular momentum states cannot be obtained as dark states due to the degenerate eigenvalue spectrum of the pseudoangular momentum operators. Instead, the degeneracy of the eigenvalue spectrum can be resolved by taking into account the nonlinearities arising from the nonvanishing Lamb-Dicke parameter associated with the laser-ion interaction. Nevertheless, it has been shown that the corresponding eigenstates of the vibrational part of the interaction Hamiltonian are very close to perfect SU(2) states for not too large values of the total pseudoangular momentum of the states.

We have used the quantum jump method to discuss the dynamical evolution of the system to a unique steady state. In such a state, the ion is decoupled from the driving laser fields and stops to radiate, and hence these states are called dark states, which are eigenstates of the interaction Hamiltonian with zero eigenvalue. We have shown both analytically and numerically that the magnitude of the Lamb-Dicke parameters associated with the quantum jumps of the driven electron plays an important role in the approach of the system to the target state.

Our method allows the preparation of SU(2) states from a manifold of initial states in a rather stable manner and does not require an initial cooling of the ion to the ground state. The prepared state is protected against degradation due to noise; the engineered Hamiltonian always pulls the state towards the target state. Of course, in order to use these entangled states in possible experiments on quantum information processing or decoherence, one should switch off the lasers after preparing the state.

ACKNOWLEDGMENTS

This work was supported by Deutsche Forschungsgemeinschaft (DFG), Deutscher Akademischer Austauschdienst (DAAD), Coordenação de Aperfeiçoamento de Pessoal de Ensino Superior (CAPES), Conselho Nacional de Desenvolvimento Científico e Tecnológico (CNPq), Fundação de Amparo à Pesquisa do Estado do Rio de Janeiro (FAPERJ), Fundação Universitária José Bonifácio (FUJB), and Programa de Apoio a Núcleos de Excelência (PRONEX).

-
- [1] P.K. Ghosh, *Ion Traps* (Clarendon, Oxford, 1995).
 [2] D.J. Wineland, R.E. Drullinger, and F.L. Walls, *Phys. Rev. Lett.* **40**, 1639 (1978).
 [3] W. Neuhauser, M. Hohenstatt, P. Toschek, and H. Dehmelt, *Phys. Rev. Lett.* **41**, 233 (1978).
 [4] D.J. Wineland and W.M. Itano, *Phys. Rev. A* **20**, 1521 (1979).
 [5] F. Diedrich, J.C. Bergquist, W.M. Itano, and D.J. Wineland, *Phys. Rev. Lett.* **62**, 403 (1989).
 [6] C. Monroe, D.M. Meekhof, B.E. King, S.R. Jefferts, W.M. Itano, and D.J. Wineland, *Phys. Rev. Lett.* **75**, 4011 (1995).
 [7] D.M. Meekhof, C. Monroe, B.E. King, W.M. Itano, and D. Wineland, *Phys. Rev. Lett.* **76**, 1796 (1996).
 [8] C. Monroe, D.M. Meekhof, B.E. King, and D. Wineland, *Science* **272**, 1131 (1996).
 [9] J.I. Cirac, A.S. Parkins, R. Blatt, and P. Zoller, *Phys. Rev. Lett.* **70**, 556 (1993).
 [10] R.L. de Matos Filho and W. Vogel, *Phys. Rev. Lett.* **76**, 608 (1996).
 [11] R.L. de Matos Filho and W. Vogel, *Phys. Rev. A* **54**, 4560 (1996).
 [12] S.-C. Gou, J. Steinbach, and P.L. Knight, *Phys. Rev. A* **55**, 3719 (1997).
 [13] S.-C. Gou, J. Steinbach, and P.L. Knight, *Phys. Rev. A* **54**, R1014 (1996).
 [14] S.-C. Gou, J. Steinbach, and P.L. Knight, *Phys. Rev. A* **54**, 4315 (1996).

- [15] J. Schwinger, in *Quantum Theory of Angular Momentum*, edited by L. Beidenham and H. van Dam (Academic, New York, 1965).
- [16] S.-C. Gou and P.L. Knight, *Phys. Rev. A* **54**, 1682 (1996).
- [17] This means that the ion will be laser driven only along the plane ($x-y$). Furthermore, as we are only interested in the motion on this plane, we can trace the density operator of the ion with respect to the vibrational state along the z direction.
- [18] G.C. Hegerfeldt and T.S. Wilser, *Proceedings of the 2nd International Wigner Symposium, 1991* (World Scientific, Singapore, 1992), p. 104; C.W. Gardiner, A.S. Parkins, and P. Zoller, *Phys. Rev. A* **46**, 4363 (1992); J. Dalibard, Y. Castin, and K. Mølmer, *Phys. Rev. Lett.* **68**, 580 (1992).
- [19] H.J. Carmichael, *An Open Systems Approach to Quantum Optics*, Lecture notes in physics (Springer, Berlin, 1993).
- [20] K. Mølmer, Y. Castin, and J. Dalibard, *J. Opt. Soc. Am. B* **10**, 524 (1993); B.M. Garraway and P.L. Knight, *Phys. Rev. A* **50**, 2548 (1994); M.B. Plenio and P.L. Knight, *Rev. Mod. Phys.* **70**, 101 (1998).